1. Introduction

For direct-cycle high-temperature reactors (HTRs) utilizing low-enriched uranium fuel, the production, release, transport and subsequent deposition of silver fission and activation products in the Main Power System (MPS) may pose maintenance problems due to excessive radiation levels to operating personnel [1]. For higher operating temperature designs, ^{110m}Ag release from fuel and deposition on high-maintenance MPS components may lead to more expensive maintenance concepts or limit planned power and outlet temperature. Accurate analyses of silver release from fuel under all expected normal operating conditions is therefore of paramount importance. Erroneous prediction of the silver source term or unnecessary uncertainties used in analyses could have serious implications for the economic case of a planned power plant. It is therefore critical that the best possible calculation model is derived from the available information.

In deriving a new, or evaluating an existing calculation model, it is important to understand the exact fuel design, fission product production, and transport through fuel materials. This could be done by considering HTR fuel sphere design, current transport models suggested, and evaluations against all available transport data. Since PBMR fuel is manufactured to be German-equivalent, PBMR may utilize German fuel programme irradiation tests as part of its fuel qualification programme to verify and validate fission product release models and parameters for its preliminary licence applications.

Historically, fission product transport through fuel materials has been considered to obey Fick's laws of diffusion through all fuel materials [2]. For silver, the limiting transport process was found to be through the SiC layer as the other fuel materials offer much less retention at reactor operating temperatures. Although it was found that SiC does not retain silver completely, it does slow down silver transport substantially [3]. Once transport behaviours through all materials have been quantified, further study was devoted to transport of silver through the SiC layer. It has been never shown that silver migrates through SiC by diffusion, but it has been assumed that the transport mechanism responsible could be approximated by a diffusion model. Various experimental studies resulted in different diffusion coefficients for silver in SiC (e.g. [1], [3] and [4]).

Due to a perceived independence on temperature, the diffusion model for silver transport through SiC has been questioned [5]. Further work led to a suggestion that silver is not transported through SiC by diffusion but by a vapour transport mechanism [6]. Although this model was questioned since it is primarily based on an absence of diffusion evidence [7], rather than on evidence of vapour transport; it does provide an alternative solution to

modelling the transport of silver in SiC. A calculation model and software were developed to perform silver release analyses from spherical fuel based on vapour transport [8]. The transport parameters required for vapour transport were derived from a first estimate evaluation of a limited set of German fuel irradiation data.

The exact transport mechanism of silver through SiC has not been resolved after 20 years of research during the German fuel development programme and now, after yet another 20 years, it is still not resolved. Other fuel qualification and characterization programmes are underway all over the world. However, it is unlikely that a solution to this problem will be found soon. In the meantime, accurate and defendable analyses of a typical PBMR core's ^{110m}Ag source term are required. This evaluation does not attempt to find the exact mechanism of silver transport, but to derive and defend a calculation model to predict the ^{110m}Ag source term under operating conditions, irrespective of the actual transport mechanisms.

1.1 Fuel Design

One of the fundamental safety requirements of modern HTRs is the ability of fuel spheres to retain fission and activation radionuclides within the fuel spheres under all expected reactor conditions. The reactor design must therefore ensure that fuel elements are never exposed to conditions in excess of their design qualification. Similarly, fuel design must make it possible for fuel elements to be manufactured economically in large volumes, while maintaining fuel quality and integrity during manufacture and subsequent irradiation.

The primary containment barrier is the Triple Coated Isotropic (TRISO) coated particle, which proved to be effective during various irradiation tests and experiments. Fission products formed in the fuel kernel either form stable oxides with oxygen released during the fission process, or have very long diffusion times through coating layers of the particle. The TRISO coated particles therefore retain fission products very effectively inside the fuel during normal operation.

Exceptions are silver and strontium fission and activation products, which do not form stable oxides at operating temperatures and have relatively fast diffusion times through coated particle layers. Fortunately, strontium has a very high sorption isotherm from graphite and is also delayed by the binder used in matrix material manufacture that significantly delays strontium release. Silver, on the other hand, has no such delaying mechanisms and is readily released from spherical fuel spheres at elevated temperatures.

Modern HTR fuel sphere design is shown in Figure 1. The design is based on the German fuel sphere design produced for the High-Temperature Reactor 500 (HTR-500) and HTR-Modul Proof Tests. This fuel type is generally regarded as state-of-the-art for German pebble fuel production [9]. It is designed for optimal performance under normal operating conditions and to withstand all design base accident conditions [10].

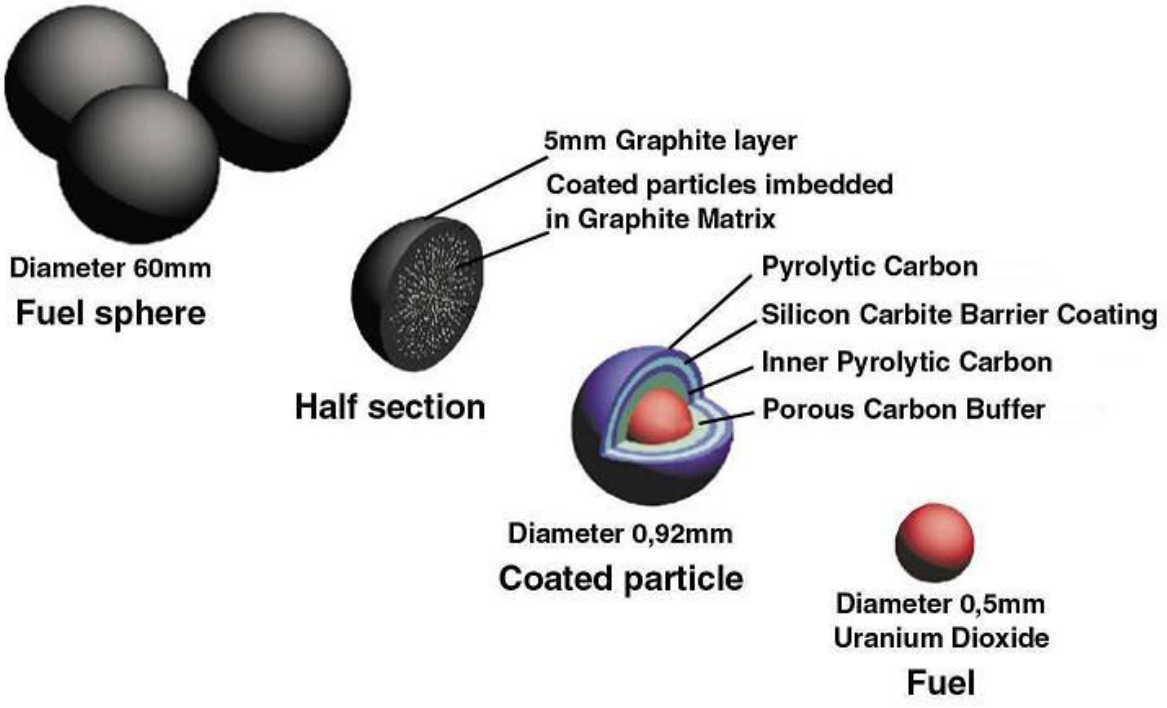

Figure 1: Fuel Element Design

Fuel spheres are manufactured from graphite matrix material (A3-3), in which TRISO coated particles are imbedded. The outer 5 mm layer contains no particles and is made up of matrix material only. The outer fuel-free zone protects the coated particles from damage from outside direct mechanical effects such as abrasion and shock. It further acts as a barrier layer against chemical corrosion in the case of water or air ingress in the core. The graphite matrix material functions as a good heat transfer medium and stabilizes the coated particles in the sphere. Good thermal contact is achieved between coated particles and matrix material, so that low temperature gradients occur in the fuel sphere.

The TRISO particle consists of a spherical UO_2-kernel, 500 micron in diameter, surrounded by four coating layers. UO_2 has a high melting point, therefore retaining its integrity under all reactor conditions. Oxygen released during fission binds with fission products to form immobile oxides. The majority of fission products are retained in the coated particle in this way. The kernel produces almost all the power of the reactor through nuclear fission. It acts as a retention barrier for gaseous fission products, thereby reducing internal pressure of the coated particle. Fission products that do not form stable oxides are released from the kernel through a diffusion process. All fission products are therefore retained or have their release reduced by the UO_2 kernel.

The kernel is surrounded by a 95-micron low-density pyrolitic carbon (PyC) layer, known as the buffer layer. This layer acts as a sacrificial layer, allowing the kernel to swell under irradiation, and providing void volume for fission gases released from the kernel. The rest of the layers are therefore protected from recoiling fission products and excessive internal pressure by the buffer layer.

The next layer is made up of dense pyrocarbon, 40 micron thick and known as the inner PyC layer. It forms an impenetrable barrier to gaseous fission products, and slows down the transport of metallic fission products to the SiC layer. During manufacture it provides a surface for the SiC to adhere to, and protects the kernel from chlorine in the form of hydrochloric acid during SiC deposition.

The SiC layer is the primary fission product barrier, being 35 micron thick. It retains all gaseous and metallic fission products to a very high extent, with the exception of silver and strontium. It provides the structural support required to contain internal gas pressure in the coated particle.

The final layer is again made of dense pyrocarbon, 40 micron thick and known as the outer PyC layer. It is under compressive stress, putting positive pressure on the SiC, helping to contain internal gas pressures. It protects the SiC layer during manufacture from chemical and mechanical damage.

To prevent coated particles from touching each other in the matrix material, which may lead to failures during the pressing stage, each coated particle is over-coated with a layer of matrix material graphite before being mixed with the bulk matrix material. Fuel spheres are pressed and machined to form perfect spheres, 60 mm in diameter.

1.2 Silver Fission and Activation Products

The main silver fission products are stable ^{109}Ag that activates to ^{110m}Ag (250 days half-life) and ^{111}Ag (7.45 days half-life). As can be seen from Figure 2, both are low-yield fission products, with cumulative fission yields from uranium of only 0.028% and 0.017% for ^{109}Ag and ^{111}Ag, respectively. For plutonium this picture changes drastically and fission yields of 1.4% and 0.30% are achieved for the two nuclides respectively. Silver release is therefore a bigger concern for high burn-up fuel where plutonium fission forms a significant fraction of the power produced in the plant. For the current PBMR design, equilibrium plutonium power fractions are in the order of 32%. For end-of-life fuel about 65% of fission power comes from plutonium fissions.

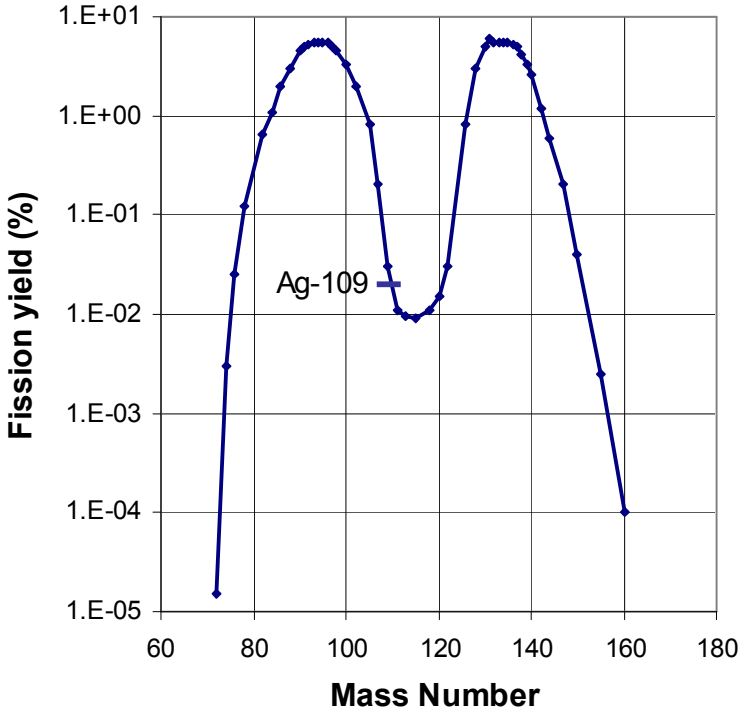

Figure 2: Thermal Neutron Fission Product Yields for ^{235}U

^{111}Ag has a relatively short half-life of only 7.45 days, and as such is only of importance during accident events. ^{109}Ag is a stable isotope, and in itself presents no danger. ^{109}Ag, however, has a large neutron capture cross section, and is activated in a neutron field to form ^{110m}Ag. Approximately 1% of the ^{109}Ag inventory is activated to ^{110m}Ag at the end of life of a fuel sphere. This includes corrections for decay and neutron capture. ^{110m}Ag is a strong γ-emitting activation product that presents a considerable radiation danger in large quantities if not shielded. With a half-life of 250 days it is released during normal operation as well as during accident events.

Most postulated accident events are dominated by ^{131}I, ^{133}I and ^{137}Cs, and to a lesser extent, ^{111}Ag and ^{90}Sr so that ^{110m}Ag is not a major contributor to public dose rates for postulated accident conditions. The main concern therefore is the production and release of ^{110m}Ag from spherical fuel elements in the reactor, and its subsequent deposition in cooler regions of the MPS, the turbine and recuperator in particular, during normal operation. Evaluation of tests and experiments conducted under conditions similar to PBMR normal operating conditions will therefore take precedence in evaluating silver release models and parameters.

1.3 Fission Production Sources

There are three distinct sources of fission products in fuel spheres:

- uranium and thorium contamination of the fuel materials;
- defective and failed coated particles; and
- intact TRISO coated particles.

These three sources and the phenomena that influence them are described below. Relative contributions to the total silver source term are based on calculations performed by a diffusion type calculation model and latest parameters suggested in the literature [2]. A fourth source also exists that is important only for activation products: The natural contamination of the activation product precursor in the fuel materials.

1.3.1 Uranium and thorium contamination of the fuel materials

Natural uranium and thorium contamination occurs in all natural materials and the raw materials used to manufacture the graphitic matrix material are no exception. This natural uranium and thorium breed fissionable plutonium and ^{233}U that in turn produce fission products. This contamination is primarily in the matrix material of the fuel sphere and release of fission products created by fissions of this contamination only have to diffuse through the matrix material before being released.

Contributions from contamination in fuel materials under normal operation conditions are only 0.2% for ^{110m}Ag and 27% for ^{111}Ag, and less than 1% for both nuclides for accident conditions. These very low relative contributions are because release from intact coated particles (that contains almost all the fissionable material) is significant. The almost negligible ^{110m}Ag contribution is due to the fact that the precursor ^{109}Ag is almost completely released from matrix material before it becomes activated to ^{110m}Ag. The only parameters that significantly influence these releases are the fuel quality specification (natural uranium, thorium and silver occurring in the matrix material) and silver diffusion coefficients in graphite. The tiny contribution to silver release under all expected conditions negates the necessity to investigate and better define this source term.

1.3.2 Defective and failed coated particles

Even under the best manufacturing conditions a small fraction of coated fuel particles will be defective. A particle is considered failed or defective if its coating layers are absent or are damaged sufficiently to allow the release of fission gases. The large-scale production experience in Germany has led to a high-quality spherical fuel element with a mean defect particle fraction of 3×10^{-5}. Furthermore, under abnormally high temperatures and power surges, coated fuel particles may start to fail. Statistical analyses of German production fuel were used to determine PBMR-manufactured fuel failure fractions. A one-sided upper 95% confidence level of 6×10^{-5} was determined. No coated particles ever failed during irradiation testing under normal operating conditions. However, due to relatively small sample sizes, failures cannot be excluded, and failure curves were derived from statistical evaluations. These expected curves and their uncertainty ranges were modelled and are used in design calculations [11]. Phenomena that may influence coated particle performance (amoeba effect, Palladium-SiC interactions, etc.) were investigated and considered where applicable [10].

Contributions from these defective and failed coated particles under normal operation conditions are 1.5% for ^{110m}Ag and 65% for ^{111}Ag. Under accident conditions contributions to ^{111}Ag release is less than 5%. The only parameters that significantly influence these releases are the fuel failure fraction and silver diffusion coefficients in UO_2 and graphite. Small contributions of ^{110m}Ag (normal operation) and ^{111}Ag (accident events) and the relative unimportance of ^{111}Ag during normal operation negate the necessity to investigate and better define this source term.

1.3.3 Intact TRISO coated particles

Whether diffusion or alternative transport models are considered, the biggest contributor to silver release from high-quality fuel is intact coated particles. Intact coated particles are defined as particles that have all their coating layers intact, are impervious to fission gas release, and release only a very small fraction of their ^{137}Cs inventory.

The contribution from intact coated particles under normal operation conditions are more than 98% for ^{110m}Ag and 8.5% for ^{111}Ag. Silver transport through SiC is the same, whether it is ^{110m}Ag or ^{111}Ag. The strong variation in ^{110m}Ag and ^{111}Ag release contribution has to do with the half-life of ^{111}Ag. The short half-life of ^{111}Ag does not allow this fission product formed in intact kernels to be released. The ^{111}Ag simply decays before it can complete its journey through the coating layers.

This is not the case during accident events, where higher temperatures reduce the breakthrough time to hours, and more than 90% of the total ^{111}Ag source term is released from intact particles.

It is therefore clear that only the diffusion coefficients and actual transport mechanisms of silver through the coating layers of an intact TRISO particle, its subsequent transport through the matrix material and desorption into the gas coolant need to be investigated and qualified in detail. The primary metallic fission product barrier layer in a TRISO particle is the SiC layer and should be the focus in modelling silver transport in and release from a fuel element. The secondary transport processes, diffusion through UO_2, PyC and matrix material and sorption on the fuel surface cannot be ignored though, and must be quantified to ensure that evaluations of SiC transport models are free from any unaccounted effects.

1.3.4 Natural contamination of activation product precursors

Some radiological important activation products have precursors that occur naturally and may be important contributors to the activation product source term. In the case of the activation product ^{110m}Ag, the precursor ^{109}Ag is a naturally occurring isotope of silver with an abundance of 48%. During low-temperature irradiation this natural contamination could dominate the ^{110m}Ag source term depending on the actual contamination level. It is difficult to measure extremely low levels of silver in fuel materials; therefore the detection limits are quite high. This causes high uncertainties of the ^{110m}Ag source terms at low irradiation temperatures. It is vital that actual silver contamination levels in fuel materials are quantified.

2. Modelling Options

2.1 Diffusion Calculation Model

The existing PBMR calculation model [12] is based on the HochTemperatur Reaktorbau (HRB) calculation model developed in Germany during the German fuel development programme. It is centred on the software product GETTER [13] and utilizes accepted transport parameters [2]. GETTER has been extensively analysed and mathematically verified to ensure that the activation product source term is calculated correctly.

2.1.1 Fission product recoil

Fission products produced during fission of fissionable isotopes recoil from their fission sites into neighbouring material. The recoil stopping range for each fission product nuclide is dependent on its mass, kinetic energy available to accelerate the nuclides from the fission site, and the material through which it penetrates. These stopping ranges determine the recoil fraction in each of the material components.

In HTR spherical fuel, the origin of this recoil is from the UO_2 kernels and natural contamination of the fuel material. Assuming a simplified isotropic geometric recoil model, the recoil release rate from a sphere of radius r_a is given by [14]:

$$R = S \cdot \pi \cdot \left(r_0 \cdot r_a^{\,2} - \frac{r_0^{\,3}}{12} \right), \qquad (1)$$

where

S is the source rate of fission products produced by fissions in material (atoms.cm^{-3}.s^{-1}) and

r_0 is the recoil range of fission product in material (cm).

Due to relatively large diffusion coefficients of silver in UO_2, the majority of ^{109}Ag formed during fission in the fuel kernel is released even at modest reactor temperatures. The contributions of recoil and knock-on effects, which are geometrical in nature, are only significant at low temperatures (< 700 °C). Under such conditions, transport through the matrix material is so slow that the silver source term is negligible in radiological terms. Recoil release is therefore included in the calculation model only for the sake of completeness.

2.1.2 Diffusion

After fission products have recoiled into neighbouring fuel materials, they are transported through the fuel materials to the surface of the fuel sphere. The calculation model assumes that fission products are primarily transported through fuel materials according to Fick's law of diffusion:

$$J_x = -D\frac{dN}{dx} \tag{2}$$

By taking into account fission product production (S) and decay terms (λc) in spherical geometry the diffusion equation becomes:

$$\frac{\partial c}{\partial t} = D\left(\frac{\partial^2 c}{\partial r^2} + \frac{2}{r}\frac{\partial c}{\partial r}\right) - \lambda c + S \tag{3}$$

The diffusion coefficient D is dependent on the temperature according to the Arrhenius equation:

$$D = D_0 e^{\frac{-E_A}{RT}}, \tag{4}$$

where

D_0 is the diffusion constant ($m^2.s^{-1}$),

E_A is the activation energy for diffusion ($kJ.mol^{-1}$) and

R is the universal gas constant, (8.3145×10^{-3} $kJ.mol^{-1}.K^{-1}$).

The diffusion equation is solved numerically for coated particles through all the coating layers, failed particles, and transport through the matrix material.

2.1.3 Surface sorption and mass transfer

The most important boundary condition used in solving the diffusion equation is the transport from the fuel surface to the coolant gas through a mass transfer coefficient that is controlled by a sorption isotherm. It is assumed that the diffusant forms a very thin gaseous boundary layer at the surface of the fuel sphere, and the convective mass transfer of the diffusant to the coolant is based on the difference between the boundary layer (C_{bl}) and coolant concentration (C_g) namely:

$$J = -D\left(\nabla c\big|_s\right) = \beta \cdot \left(c_{bl} - c_g\right), \tag{5}$$

where

J is the flux of material transfer at the surface,

$\nabla c\big|_s$ is the concentration gradient of diffusant at the fuel sphere surface, and

β is the mass transfer coefficient,

which is calculated from analogous correlations used for heat transfer, by substitution of the Nusselt and Prandtl numbers with the Sherwood (Sh) and Schmidt (Sc) numbers respectively, so

$$\beta = \frac{Sh \cdot D_g}{d}, \text{ and} \tag{6}$$

$$Sh = 1.27\frac{Sc^{1/3}}{\varepsilon^{1.18}}Re^{0.36} + 0.033\frac{Sc^{1/2}}{\varepsilon^{1.07}}Re^{0.86}. \tag{7}$$

For low diffusant boundary layer pressures and high temperatures, the concentration in the boundary layer is related to the partial pressure (p_{bl}) by the ideal gas relation

$$c_{bl} = \frac{p_{bl}}{RT}N_A, \tag{8}$$

where

N_A is Avogadro's number, (6.022 x 10^{23} mol^{-1}) and

R is the universal gas constant (8.3145 $dm^3.Pa.mol^{-1}.K^{-1}$).

The partial pressure in the boundary layer is determined from the Henry or Freundlich isotherms [2], which give the relationship between partial pressure and matrix surface concentration. The transition from dominant Henry to dominant Freundlich isotherms occurs at very high surface concentrations (>0.1μmol.g^{-1}), which are rarely attained under normal operation conditions.

The partial vapour pressure is a function of the surface concentration and temperature, and is calculated as the sum of the Henry and Freundlich isotherm vapour pressure:

$$p = p_H + p_F\,, \tag{9}$$

where

$$p_H = c_s \exp\left(\left(A + \frac{B}{T}\right) + \left(D - 1 + \frac{E}{T}\right)\ln c_t\right), \tag{10}$$

$$p_F = \exp\left(\left(A + \frac{B}{T}\right) + \left(D + \frac{E}{T}\right)\ln c_s\right) \text{ and} \tag{11}$$

$$\ln c_t = d_1 - d_2 T\,. \tag{12}$$

The constants A, B, D, E, c_1, d_1 and d_2 are empirically derived, where

T is the surface temperature in K,

p_H is the Henry isotherm vapour pressure in Pa,

p_F is the Freundlich isotherm vapour pressure in Pa,

B and E are constants in K,

c_s is the concentration on surface in μmol.gC^{-1} (micromole per gram carbon) and

d_1 and d_2 are constants in K^{-1}.

Simplifications of the above formulae may be made by combining expressions containing constants into new constants. This is especially true for the low concentration Henry region; the correlation can be written as [14]:

$$p_H = c_s \exp\left(E + \frac{1000 \bullet E2}{T}\right) \tag{13}$$

2.2 Molecular Vapour Transport Release Calculation Model

An alternative model, the Molecular Vapour Transport Release Model [8], has been suggested that assumes diffusion transport through all fuel materials except the SiC layer. In this model it is hypothesized that Ag leaks through Nano-Tube Failures (NTF) in the SiC layer from the IPyC to the OPyc layer. Different flow regimes exist depending on the sizes of the NTF and molecule, gas pressure, flow velocities and temperature. Whether molecules travelling through the NTF interact primarily with the walls of the flow channel (molecular flow) or with other molecules in the flow channel (viscous flow), depends primarily on the pressure in the system.

The limits between molecular, transitional, and laminar flow is defined by the Knudsen number, which is the ratio of the mean free path of a molecule to a characteristic dimension of the channel, usually the tube diameter, through which the gas is flowing [6].

$$Kn = \frac{\lambda}{d}, \tag{14}$$

where

λ is the mean free path (m) and

D is the channel diameter (m).

For an ideal gas the mean free path is:

$$\lambda = \frac{RT}{\sqrt{2}\pi d^2 N_A P}, \tag{15}$$

where

R is the universal gas constant (8.3145 J.mol^{-1}.K^{-1}),

T is theTemperature (K),

d is the channel diameter (m),

N_A is Avogadro's number (6.022 x 10^{23} mol^{-1}),

P is the Pressure (Pa).

The gas pressure in the SiC is very low due to the inner PyC layers retaining all fission gases and CO_2 formed in the kernel and buffer layers. The mean free path of gas molecules is much larger than the dimensions of the nano-tubes, therefore molecular flow is the dominating flow regime and viscous or transitional flow are not considered. For molecular flow the following mass transfer equation can be applied [6]:

$$Q_m = \frac{C_m \Delta t}{V_{molar}} M_{molar}, \tag{16}$$

where

Q_m is the mass transfer over time Δt [g],

V_{molar} is the molar volume [$m^3.mol^{-1}$],

M_{molar} is the atomic mass [$g.mol^{-1}$] and C_m is the conductance [$m^3 s^{-1}$].

The conductance is calculated by:

$$C_m = \frac{d^3}{6L}\sqrt{\frac{2\pi RT}{M_{molar}}}, \tag{17}$$

where

d is the nano-tube circular diameter (m) and

L is the nano-tube length (m).

All nano-tubes are assumed to be straight tubes with circular cross sections with the length of each tube equal to the SiC coating thickness. This calculation model calculates transport from UO_2 kernels and through PyC and matrix material similarly to the diffusion calculation model. Since this model has only been used to evaluate experiments and reactor conditions where centre fuel temperatures exceed 900 °C, it ignores recoil effects and sorption from the fuel surface. Should the molecular vapour transport release model be further developed in future, recoil and sorption effects will have to be included, but the effect on total core release from a typical planned HTR operating with reactor outlet temperatures exceeding 900 °C will be small.

3. Evaluation of Material Tests

Material tests are usually separate effect tests that focus on only one or maybe two phenomena at a time. A particular parameter can then be appraised and possibly quantified in order to simplify the assessment of integral effects tests later on. Specific material tests are evaluated first to ensure that all parameters are quantified as well as possible before integral effect evaluations of full sphere irradiation tests are performed.

3.1 Sorption Isotherms

Few attempts have been made to determine silver sorption isotherms during the German fuel programme. Standard procedure such as isopiestic methods [15] did not yield good results due to low sorption of silver on matrix materials. Silver sorption from matrix materials has in general just been ignored in the available literature. The caesium sorption isotherm, on the other hand, has been studied very well and is described in detail in the literature [16]. Sorption isotherms for both Freundlich and Henry regions on a large variety of nuclear graphite have been derived in a Knudsen cell mass spectrometer system for caesium but not for silver [17].

The only silver sorption investigation performed that was published in the literature [18] did not provide sorption isotherms, but did show desorption spectra of caesium and silver using an identical experimental setup and test conditions. The desorption spectra are shown in Figure 3 verbatim. The technique is known as Temperature Programmed Desorption (TPD). It consists of measuring the rate of desorption from a surface as its temperature is increased linearly with time. A monolayer of caesium and silver is evaporated onto the surface of a test sample, and then heated at a constant rate. The desorption rate is presented as a fraction of the highest rate achieved, which is also the point where all the available atoms have been released from the surface. A broadening tail after the caesium peak is observed, which are most likely atoms that have diffused into the porous matrix material, and have a delayed release mechanism.

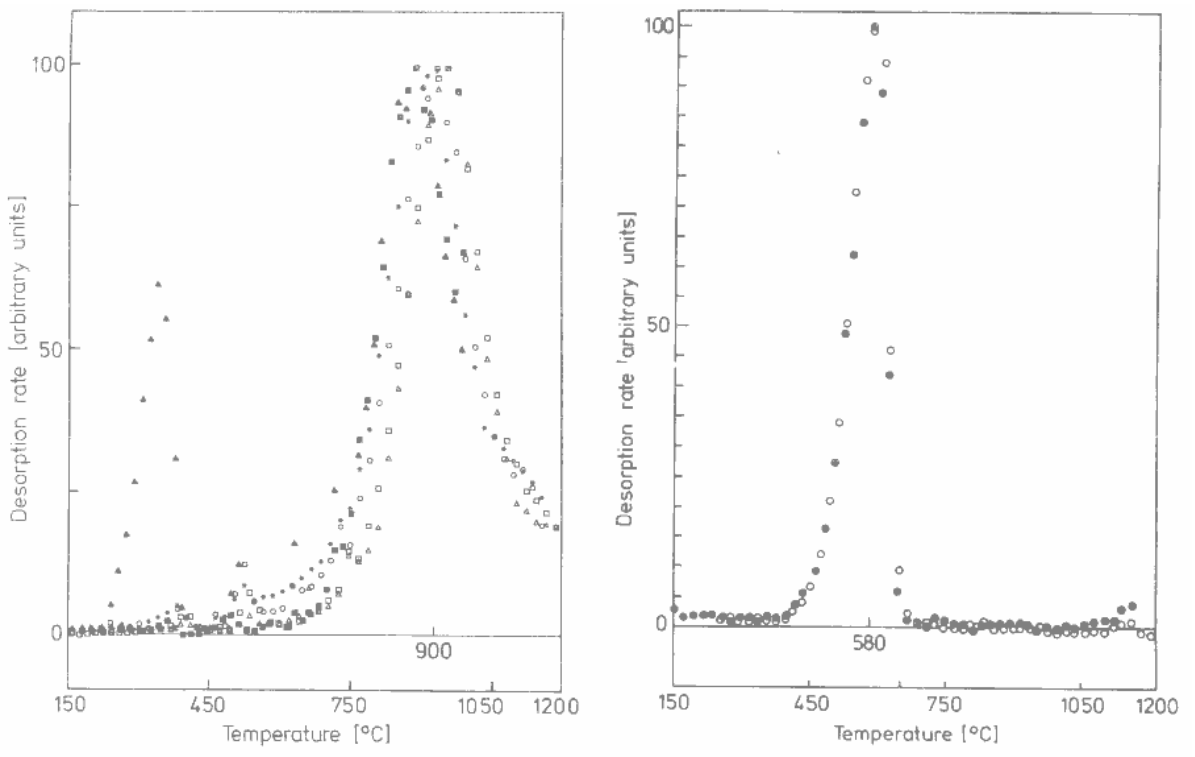

Figure 3: Experimental Desorption Spectra of Caesium (left) and Silver (right)

Several experiments are plotted on each graph. The first graph shows the caesium desorption spectra. The peak at ~320 °C in the first graph corresponds to a test performed under oxidizing conditions and should be ignored. The first graph shows that caesium starts to desorb at approximately 500 °C. The maximum desorption rate occurs at ~890°C, but that is due to the fact that the caesium atoms deposited onto the matrix material surface are depleted and no more atoms are available to be measured. Should there be an 'infinite source' of caesium inside the sample material, a peak would not be observed but a curve where the desorption rate approaches a maximum depending on how fast caesium atoms are supplied to the surface of the sample. This is exactly the case when this data is evaluated with a fuel transport code utilizing sorption models such as found in GETTER.

The second graph shows silver desorption rates under the same conditions as some of the caesium spectra. Silver starts to desorb from the surface at approximately 400 °C and peaks at 580 °C. What is immediately obvious is that silver desorbs at much lower temperatures than caesium, and this also explains why it is relatively difficult to estimate silver sorption isotherms using isopiestic methods. These graphs show that matrix material sorption is a significant retention mechanism for caesium and silver for temperatures up to 1 000 °C and 700 °C respectively, after which desorption from the fuel surface occurs so quickly that it has a negligible effect on overall fuel release.

An attempt was made to evaluate these desorption spectra with the sorption isotherms used in GETTER [13]. The caesium fractional release with a desorption rate using the known sorption isotherms was compared with the fractional release when graphite sorption was set to almost zero. This was achieved by setting the sorption isotherms *E* and *E2* defined in paragraph 2.1.3 to their accepted values of 10.44 and -41.9 K first to simulate real sorption and then setting *E* (dimensionless parameter) so high (1 000x partial pressure) that sorption becomes negligible in the temperature region under consideration. The GETTER desorption rate curve and the experimental curve are shown in Figure 4 with desorption temperature (^{o}C) and rate (arbitrary units) axis. The maximum GETTER desorption rate is achieved at 1 150 °C after which sorption has no effect on caesium release. At the maximum experimental desorption rate temperature, the GETTER desorption rate is 66% of the maximum desorption rate.

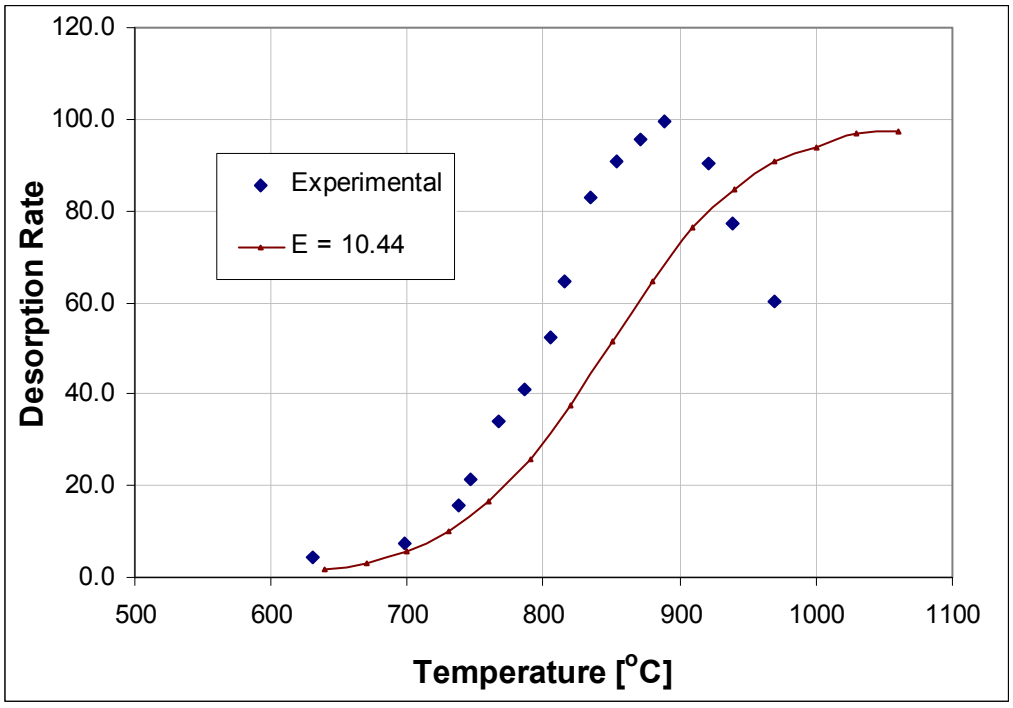

Figure 4: Cs sorption: Experimental vs. GETTER Sorption Isotherm

The GETTER evaluation above was repeated for silver experimental results. Caesium results could then be used as a benchmark to determine a realistic silver sorption isotherm. This is of course assuming that the same desorption model applies to both caesium and silver, and that the caesium sorption isotherm is correct for this experiment. Previously the HRB approach to modelling silver sorption was to assume that the silver partial pressure is a hundred times higher than the caesium partial pressure [13]. The sorption isotherm *E2* was kept constant and the *E* sorption isotherm was increased to 12.74.

Curves that were conservative for lower temperatures could be obtained by keeping the sorption isotherm *E2* constant as per the HRB approach and further increasing the dimensionless *E* sorption isotherm. In Figure 5 silver experimental desorption rates are compared with GETTER calculated desorption rates for the sorption isotherm *E* set to 16, 17 and 18. In all cases the maximum desorption rate was achieved at about 720 °C. When the dimensionless sorption isotherm *E* is set to 17, GETTER calculates a desorption rate (with arbitrary units) of 66% of the maximum desorption rate at the maximum experimental desorption rate temperature. This compares with the caesium sorption evaluation using best available sorption isotherms. It is therefore recommended that values of 17 and -41.9 K be used for *E* and *E2* respectively for best estimate analyses and 18 and -41.9 K for design limit calculations.

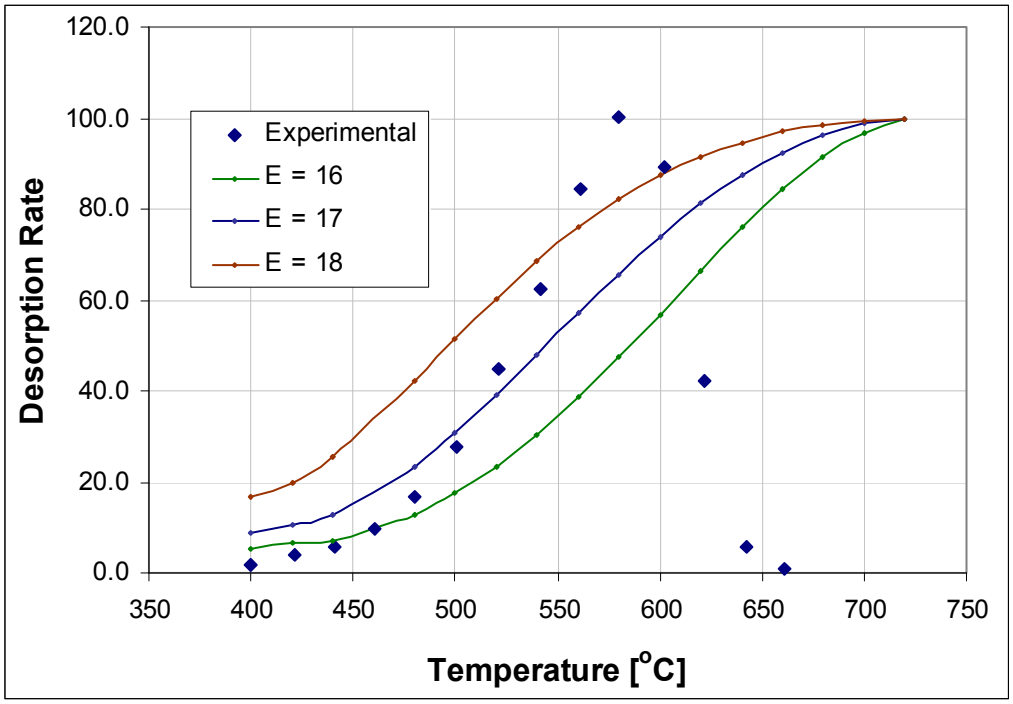

Figure 5: Ag Sorption: Experimental vs. GETTER Sorption Isotherm

The newly derived and HRB sorption isotherms' effect on silver partial pressures at different surface concentrations are shown in Figure 6. The new sorption isotherms increase the silver partial pressures by a factor of 70. Most modern high-temperature gas-cooled reactor designs are planned to operate with reactor outlet temperatures between 750 °C and 950 °C. It can therefore be argued that the silver sorption isotherm is only of academic importance, and will not influence the total ^{110m}Ag source term significantly. It is, however, still important to show that all phenomena have been considered and that similar calculation models are employed for all radiological significant nuclides.

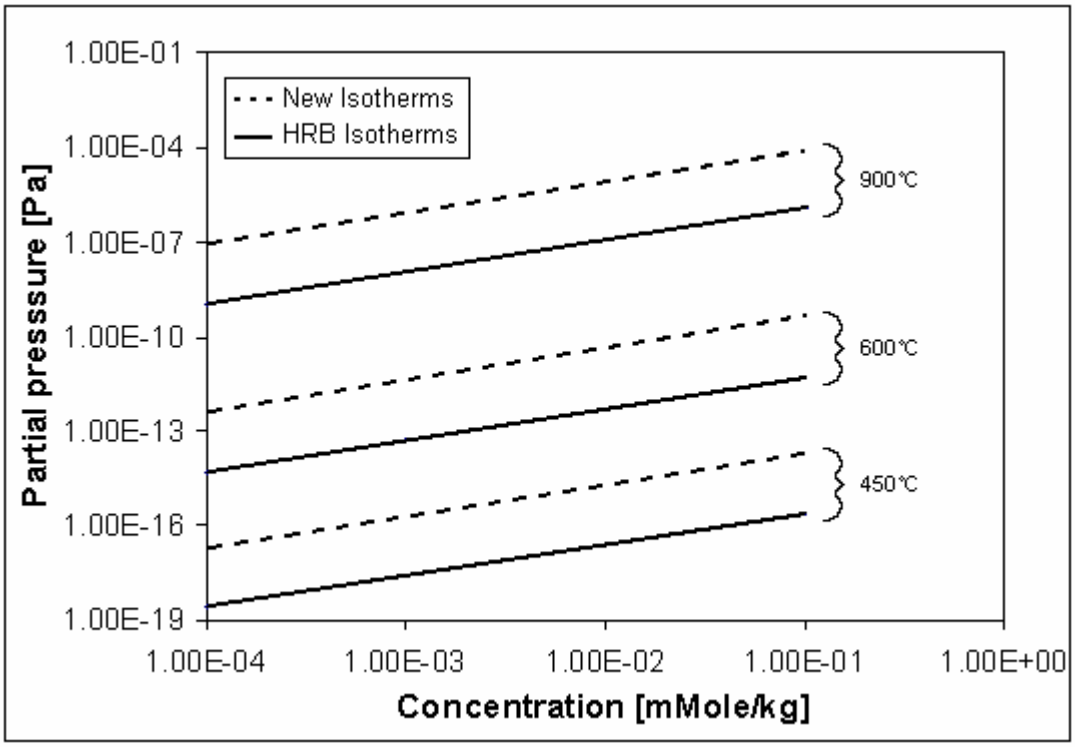

Figure 6: Old and New Ag Sorption Isotherms on A3-3 Matrix Graphite

3.2 Matrix Material Transport

Transport of silver through graphitic matrix material has been investigated in detail in [19] and [20]. The diffusion of silver in original, oxidized and fast neutron irradiated A3-3 and in original A3-27 matrix materials were studied in vacuum by measuring the ^{110m}Ag release kinetics and concentration profiles from cylindrical samples.

The release kinetics and concentration profiles both satisfied Fick's law of diffusion and diffusion coefficients for temperatures between 800 °C and 1 300 °C were derived [20]. Since PBMR is only considering A3-3 equivalent matrix material for its demonstration plant's fuel, only A3-3 diffusion coefficients will be evaluated. Silver retention in A3-3 matrix material increases with irradiation up to ~7 displacements per atom (equivalent to a fast neutron fluence of approximately 5 x 10^{25} m^{-2}). Diffusion coefficients show typical Arrhenius behaviour where R is the universal gas constant (8.3145 x 10^{-3} kJ. $mol^{-1}.K^{-1}$) and T is the absolute temperature.

Original A3-3: $D = 6.80 \times 10^{1} e^{-262/RT}$ $m^2 s^{-1}$

Irradiated A3-3: $D = 1.60 \times 10^{0} e^{-258/RT}$ $m^2 s^{-1}$

Pebble fuelled HTRs employ dynamic core loading schemes so that an equilibrium core contains from fresh fuel to highly irradiated spent fuel. For best estimate analyses, the irradiated diffusion constant and activation energy has been used. This can be justified as the ^{110m}Ag inventory is small in the beginning of a sphere's irradiation life and releases are modest due to the fact that the ^{235}U fission yield for ^{109}Ag is very small. Later in a sphere's life when the matrix material is highly irradiated, the ^{110m}Ag inventory grows very quickly as high silver yield ^{239}Pu and ^{241}Pu fission contribution becomes significant. For best estimate analyses this may be fair, but for safety analyses design calculations, a more conservative approach is required.

In Figure 7 diffusion coefficients for both original and irradiated A3-3 matrix material is plotted against temperature. It may be overly conservative to simply assume the fastest diffusion coefficient for safety analyses. A more fitting approach would be to assume that irradiation effects have a linear effect on the silver retention ability of A3-3 matrix material. It will still be conservative in the sense that the high inventory and highly irradiated end-of-life fuel will have faster silver transport than experimentally measured.

However, the fresh fuel release (although several factors less than end-of-life fuel release) will not be underestimated. The suggested PBMR design diffusion constant is plotted in Figure 7. The recommended best estimate and design silver diffusion coefficient is thus:

PBMR best estimate $: D = 1.60 \times 10^{0} e^{-258/RT}$ $m^2 s^{-1}$

PBMR design : $D = 1.10 \times 10^{1} e^{-260/RT}$ $m^2 s^{-1}$

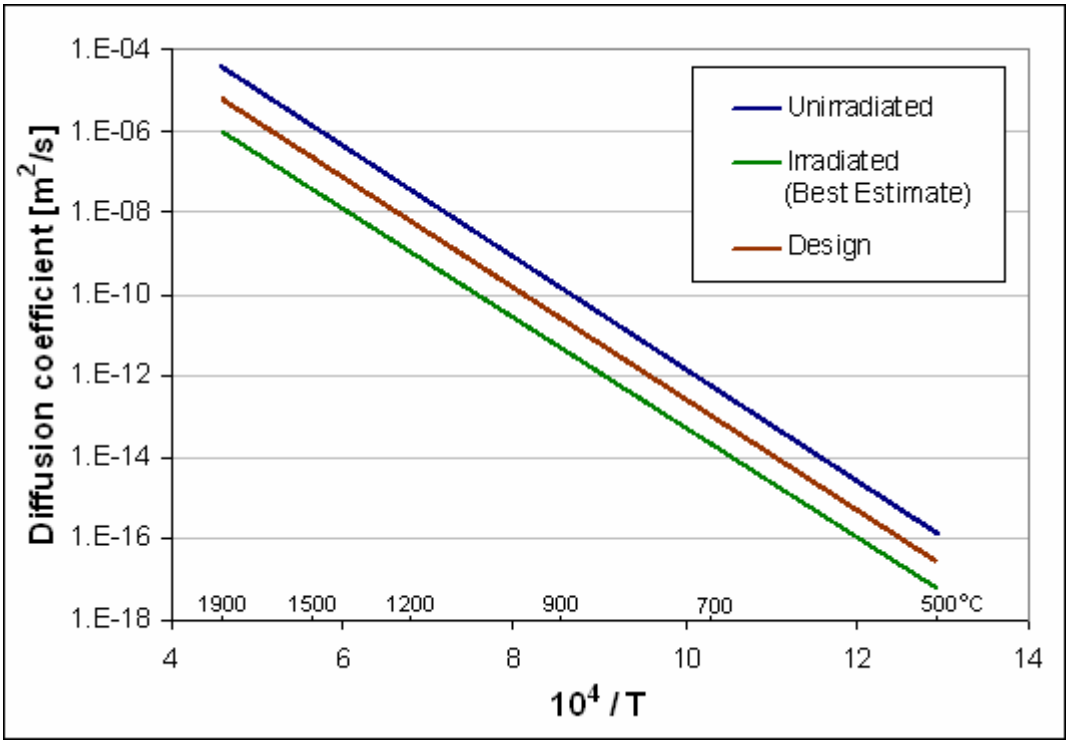

Figure 7: Silver Diffusion Coefficient in the Matrix Material

3.3 Coated Particle Transport

The transport of silver through coating layers of a coated particle has been studied in depth by many researchers [2]. Compared to transport through the SiC layer, transport through the UO_2 kernel and PyC layers are relatively quick. The diffusion coefficients of silver in the UO_2 kernel and PyC layers are 200 and 500 times larger than in SiC at 1 000 °C. Both German and United States fuel development programmes suggested the same diffusion coefficients for best estimate analyses for UO_2 kernel and PyC layers [2].

Best estimate UO_2: $D = 6.70 \times 10^{-9} e^{-165/RT}$ m^2s^{-1}

Best estimate PyC: $D = 5.30 \times 10^{-9} e^{-154/RT}$ m^2s^{-1}

For safety analyses to determine design limits, an uncertainty for the above diffusion constants of a factor of two was suggested before [21]. This uncertainty, or even more conservative safety factors, has only a small effect on the overall silver release rate.

The most efficient barrier to the release of silver in an HTR fuel element remains the SiC layer and it has been studied in detail (e.g. [1], [2], [3] and [6]). Nabielek *et al*. measured silver release by gamma-ray spectrometric measurements of fuel tubes and other graphite components from a variety of fuel particles during irradiation and post-irradiation heating tests between 850 °C and 1 500 °C. An effective diffusion coefficient for silver in silicon carbide was derived:

Nabielek *et al*. [1]: $D = 6.76 \times 10^{-9} e^{-213/RT}$ m^2s^{-1}

Silver and caesium release from loose particles that had been previously irradiated in compacts or test spheres were measured by Amian and Stöver during heat-up tests [3]. Irradiation temperatures varied from 400 °C to 1 050 °C and burn-ups between 2.3% and 12.1% Fissions per Initial Metal Atom (FIMA) with fast fluences between 0.5×10^{25} m^{-2} to 8.2×10^{25} m^{-2} were achieved. Annealing temperatures between 1 000 °C and 1 500 °C were used for up to 2 340 hours. Different particle types had different fuel kernel materials with slight variations in coating dimensions. Diffusion coefficients for silver in silicon carbide was derived for all types of kernels (UO_2, UC_2, ThO_2, mixtures, etc.) and for reference quality fuel (UO_2, $(U,Th)O_2$) and published in [3]:

All fuel types: $D = 4.5 \times 10^{-9} e^{-218/RT}$ m^2s^{-1}

Reference fuel only: $D = 3.6 \times 10^{-9} e^{-215/RT}$ m^2s^{-1}

Both research efforts found scatter up to one order of magnitude of the diffusion coefficient at any temperature. Silver is released from particles that retain caesium, which means from coated particles with intact SiC layers, but ion implantation experiments suggest that silver does not undergo bulk SiC diffusion [1]. This anomaly was resolved by suggesting that implanted silver is stopped primarily in the SiC grains, while fission product silver in a fuel element is transported along crystal grain boundaries which contain traces of free silicon [3]. Free silicon is a function of coating conditions and it goes a long way to describe the scatter in the experimentally measured silver diffusion coefficients. Grain boundary diffusion depends on the exact microstructure of the sample, which varies from sample to sample. Accordingly, activation energies for diffusion in pyrolytically deposited SiC coatings are approximately 200 kJ/mol while the activation energies for diffusion in single crystals are about 450 kJ/mol.

Other studies did not agree, as the scatter in the reported data exceeds the expected variations in SiC structure and the silver path length travelled through the SiC coatings [6]. From ion implantation studies [5] and diffusion couple investigations [22] an alternative transport mechanism that entails transport of silver though cracks in the SiC layer were suggested. From this mechanism a model was derived and used to perform an estimate of silver release from a typical PBMR core based on a first estimate of some German irradiation data [8].

Measurements made on loose particles remain problematic. The silver inventory in a single particle is very small and measurement errors on such small activities continue to be challenging. Furthermore, it must be asked if packing into a sphere and high-temperature heat treatment during final annealing of fuel spheres do not affect coated particle characteristics. Measurements in material samples only also remain problematic. Geometric effects, irradiation fluxes and temperatures cannot be repeated and these effects on silver transport cannot be comprehended.

The exact SiC transport mechanism cannot be derived from the available material test data. Innovative and new material tests must be invented and performed to understand the exact mechanism. Considering tests and experiments already performed, which yielded varying results and contradicting mechanisms, it seems unlikely that clear proof will be available any time soon. The only recourse in the meantime is to evaluate all the available real data, in other words, the actual measured release from complete fuel spheres under conditions that are similar to expected reactor conditions.

3.4 Material Test Evaluation Discussion

Transport phenomena investigated in material tests can be divided into two groups:

- A secondary effects group that only has a limited consequence on the silver release source term. These include recoil, diffusion transport through UO_2, PyC and matrix material, and sorption on the fuel surface. These phenomena have either negligible effects (recoil and sorption) or are very well understood (diffusion through UO_2, PyC and matrix material) and do not have a controlling function on silver release.
- A primary effects group is phenomena that control silver release under most reactor conditions considered. In this case, it is only silver transport through SiC which is also the least understood phenomenon. In order to derive the best calculation model to predict the ^{110m}Ag source term, secondary transport phenomena are assumed to be correct, based on separate effects materials tests evaluated in Chapter 3, and the primary effect, SiC transport, is evaluated by integral effects of irradiation tests in Chapter 4.

4. Evaluation of Irradiation tests

4.1 Selection of Irradiation Tests

A study of all available irradiation tests has been performed [23] and applicable tests that might be used to derive silver transport models and parameters have been described. Table 1 shows all applicable irradiation tests to be considered. All values in Table 1 are as reported in the literature before any evaluation has been performed. Temperatures and fluences are often pre-irradiation targets and burn-ups are first-calculated estimates. All tests are listed from most applicable to least applicable. Applicability in this case is defined according to fuel type, irradiation conditions and availability of irradiation data and silver fractional release results.

4.1.1 Fuel type

Ideally, considered irradiation tests must have tested fuel containing low enriched UO_2 TRISO coated particles, where coating layers are as close as possible to that of the PBMR fuel design [10]. Due to low retention of silver in kernel and graphite materials, and for the purpose of this study, the nature of the kernel and pyrocarbon layers is not considered as an inhibitive factor for evaluation of an irradiation or heat-up test. Therefore, UC_2- and Th-based fuels and matrix materials other than A3-3 may be considered. For the same reason, non-spherical fuel such as compacts may be considered as well, but the geometry must be taken into account. Additionally, coated particle failure and defect fractions must be more than a factor of ten lower than the fractional release of silver in a test. This is to ensure that silver release evaluations are governed by silicon carbide retention.

4.1.2 Irradiation history

Irradiation history refers to the availability of data (such as time-dependent temperatures, release rates of fission gases, neutron fluxes, etc.) describing irradiation conditions which coated particle fuel in the test were exposed to. Ideally the irradiation history must be comparable with expected reactor conditions considered and detailed data sets must be available.

Unfortunately much of the detailed German data have been lost or are very difficult to find. In some cases only ‘single values’ could be found, for example, a single maximum fuel temperature rather than all the temperatures measured during irradiation.

Where complete irradiation histories are unavailable, an evaluation can still be performed by assuming steady state irradiation conditions, but this is of course much less satisfactory. Often the only option is to make a conservative assumption that adds extra uncertainty in the final result.

Sometimes irradiation history data is presented as graphs in documents, typically surface temperature, burn-up (% FIMA), and release rates of gaseous isotopes. The origin of these graphs is from tabulated data, which is often unavailable. The raw data may be estimated from these graphs using opto-digital software.

Thermal fluxes can be back-calculated quite accurately from the burn-up history (% FIMA) of the fuel, and this can be done quite precisely if final inventories of some isotopes in the fuel element are available. The most important irradiation history parameter required is the fuel temperature, as evaluations matching fractional releases do not require accurate estimates of the inventory. Fast neutron dose (irradiation damage) has recently come under consideration as a factor affecting silver retention in silicon carbide and influencing thermal conductivity in fuel materials. In most cases the history of this dose is relatively linear in nature, and easily estimated once final values are known.

4.1.3 Fractional release data

If the fractional release of silver could not be found in the literature, there is little point in carrying out the irradiation evaluation. In some cases, silver released from a sphere is given as an absolute amount, and it is necessary to calculate the total silver inventory from burn-up. Other times, silver profiles are given, either in the complete sphere, or just in the fuel-free zone. Here an evaluation can still be performed for some models, but deriving transport parameters becomes questionable.

The availability of fractional release rates for other radionuclides is very valuable in evaluating silver fractional release data. Release over birth ratio (R/B) for krypton fission gases are valuable indicators of coated particle performance and caesium fractional release rates indicate the quality of SiC layers.

Fractional releases of above irradiation tests for ^{110m}Ag, ^{134}Cs, ^{137}Cs and end-of-life release over birth ratio (R/B) of ^{85m}Kr is graphically presented in Figure 8.

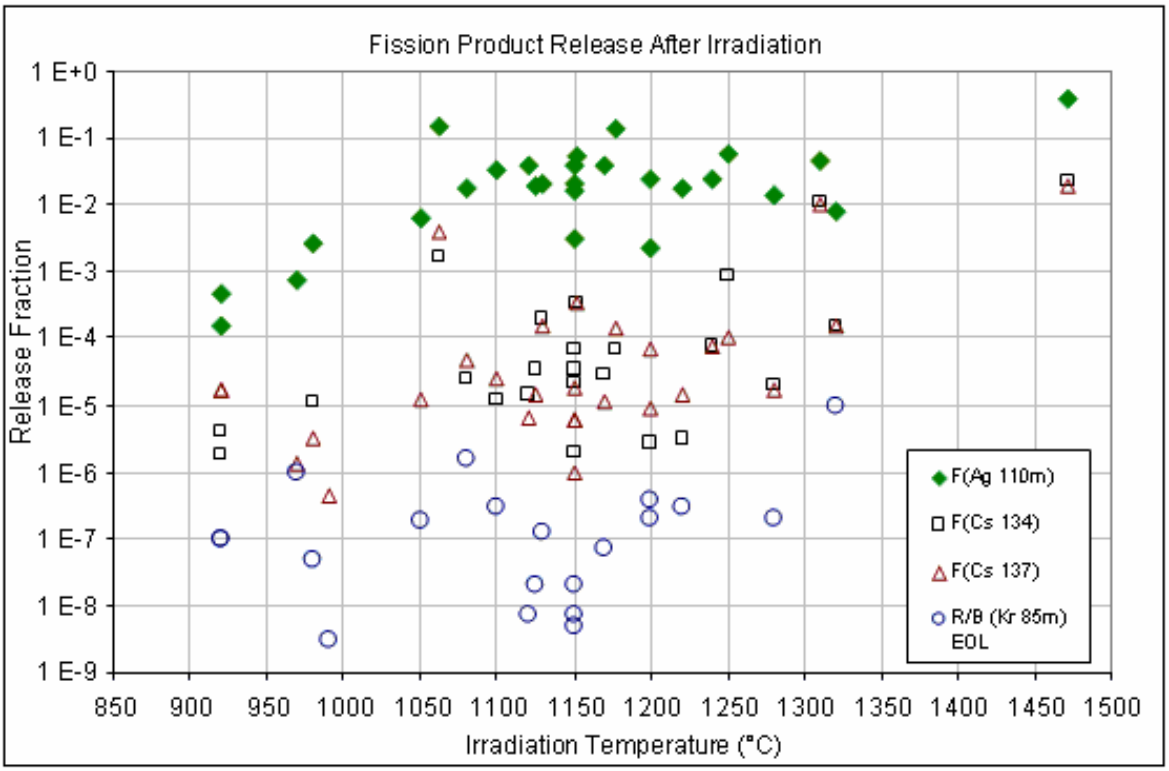

Figure 8: Fractional Release of Fission Products after Irradiation

In Table 1 considered irradiation tests are divided into three groups:

- Highly applicable irradiation tests' evaluations can be carried out relatively quickly on most models currently used for silver transport, as sufficient information is available, and a good degree of certainty is ensured by many literature sources. Transport parameters derived from these evaluations must be considered the most valuable and weigh the most in terms of importance.
- Medium applicable irradiation tests' evaluations should basically be done after the high priority set, as some more data may be needed, or additional work needs to be carried out that would take much longer than a high priority evaluation. Derived transport parameters must be considered less important than the high applicable results.
- Low applicable irradiation tests' evaluations would typically take much longer than other evaluations and need a significant amount of source information. Assumptions have to be made that would reduce the value of derived transport parameters and therefore should have the lowest weight when final transport parameters are considered. Many other irradiation tests have been considered as well but rejected as significant data is missing, could not be sourced, and in some cases was not even measured.

Table 1: Considered Irradiation Tests

Experiment	Irradiation Time (EFPD)	Maximum Fuel Temperature	Burn-up % FIMA	R/B ^{85m}Kr	Fractional ^{110m}Ag Release	Fractional ^{137}Cs Release	Fuel Type
High Applicability							
HFR-K3/1	359	1 200 °C	7.5	2×10^{-7}	2.2×10^{-3}	9.1×10^{-6}	UO_2 fuel reload 19
HFR-K3/2	359	920 °C	10	1×10^{-7}	4.5×10^{-4}	1.7×10^{-5}	UO_2 fuel reload 19
HFR-K3/3	359	920 °C	10.6	1×10^{-7}	3.2×10^{-4}	1.7×10^{-5}	UO_2 fuel reload 19
HFR-K3/4	359	1 220 °C	9	3×10^{-7}	1.8×10^{-2}	1.4×10^{-5}	UO_2 fuel reload 19
FRJ2-K13/1	396	1 125 °C	7.5	2×10^{-8}	1.9×10^{-2}	1.4×10^{-5}	UO_2 fuel reload 19
FRJ2-K13/2	396	1 150 °C	8	2×10^{-8}	2.0×10^{-2}	1.8×10^{-5}	UO_2 fuel reload 19
FRJ2-K13/3	396	1 150 °C	7.9	7×10^{-9}	1.7×10^{-2}	6.1×10^{-6}	UO_2 fuel reload 19
FRJ2-K13/4	396	1 120 °C	7.6	7×10^{-9}	3.9×10^{-2}	6.4×10^{-6}	UO_2 fuel reload 19
FRJ2-K15/1	533	970 °C	14.1	1×10^{-6}	7.5×10^{-4}	1.3×10^{-6}	UO_2 fuel reload 21
FRJ2-K15/2	533	1 150 °C	15.3	5×10^{-9}	3.2×10^{-3}	9.5×10^{-7}	UO_2 fuel reload 21
Medium Applicability							
R2-K13/1	517	1 170 °C	10.2	7×10^{-8}	3.9×10^{-2}	1.1×10^{-5}	UO_2/Th fuel
R2-K13/4	517	980 °C	9.8	5×10^{-8}	2.7×10^{-3}	3.2×10^{-6}	UO_2/Th fuel
R2-K12/1	308	1 100 °C	11.1	3×10^{-7}	3.3×10^{-2}	2.4×10^{-5}	UO_2/Th fuel
R2-K12/2	308	1 280 °C	12.4	2×10^{-7}	1.4×10^{-2}	1.7×10^{-5}	UO_2/Th fuel
FRJ2-K11/3	260	1 150 °C	11.5	-	4.0×10^{-2}	6.0×10^{-6}	UO_2/Th fuel
FRJ2-K11/4	260	1 152 °C	8.5	-	5.4×10^{-2}	3.3×10^{-4}	UO_2/Th fuel

Experiment	Irradiation Time (EFPD)	Maximum Fuel Temperature	Burn-up % FIMA	R/B ^{85m}Kr	Fractional ^{110m}Ag Release	Fractional ^{137}Cs Release	Fuel Type
Low Applicability							
R2-K12/3	308	1 200 °C	10.3	4×10^{-7}	2.4×10^{-2}	6.8×10^{-5}	UC_2/Th fuel
R2-K12/4	308	1 050 °C	11.8	2×10^{-7}	6.3×10^{-3}	1.2×10^{-5}	UC_2/Th fuel
FRJ2-K10/3	291	1 250 °C	73	-	5.6×10^{-2}	1.0×10^{-4}	UC_2 fuel
FRJ2-K10/4	291	1 240 °C	70	-	2.5×10^{-2}	7.5×10^{-5}	UC_2 fuel
FRJ2-P27/1	232	1 080 °C	7.6	2×10^{-6}	1.8×10^{-2}	4.7×10^{-5}	Compact U fuel
FRJ2-P27/2	232	1 320 °C	8	1×10^{-5}	8.2×10^{-3}	1.5×10^{-4}	Compact U fuel
FRJ2-P27/3	232	1 130 °C	7.6	1×10^{-7}	2.0×10^{-2}	1.6×10^{-4}	Compact U fuel
FRJ2-P23/1	177	1 250 °C	12.5	-	1.5×10^{-1}	3.9×10^{-3}	Compact Th fuel
FRJ2-P23/2	177	1 210 °C	12.5	-	1.4×10^{-1}	1.4×10^{-4}	Compact Th fuel
FRJ2-P23/3	177	1 472 °C	11.9	-	4.0×10^{-1}	1.9×10^{-2}	Compact Th fuel
FRJ2-P23/4	177	1 310 °C	12.1	-	4.6×10^{-2}	9.9×10^{-3}	Compact Th fuel
BR2-P21/1	380	1 350 °C	9	-	1.1×10^{-1}	7.6×10^{-2}	Compact U fuel
BR2-P21/2a	380	1 550 °C	10	-	2.2×10^{-1}	7.6×10^{-2}	Compact Th fuel
BR2-P21/2b	380	1 550 °C	9		6.0×10^{-2}	3.0×10^{-2}	Compact Th fuel
BR2-P22/2	257	1 350 °C	6	-	5.0×10^{-3}	2.1×10^{-3}	Compact Th fuel

4.2 Molecular Vapour Transport Release Model

A first analysis was performed to evaluate the ^{110m}Ag source term for a typical PBMR core design [24]. Readily available German irradiation test data was used in a calculation model that could utilize both diffusion and MVR transport through SiC layers [8]. The evaluation performed did not attempt to establish whether the MVR transport mechanism is a valid physical explanation for silver transport through SiC, but only assessed the ability of the model to reproduce real experimental results. Two statistical quantities are required for MVR analyses: nano tube failures (NTF) and the total nano-tube cross-sectional surface. For example, an NTF of 10% would mean that 10% of 14 400 particles in a sphere would release Ag through nano-tubes and the other 90% would fully contain all Ag inside the particle. NTF is a statistical quantity since it could vary from sphere to sphere depending on the reasons for the existence of nano-tubes. NTF can be determined from observed Ag release fractions from available test data if the nano-tube cross-sectional surface is known or fixed.

Since NTF has never been observed in coated fuel particles, it is impossible to know the value of the cross-sectional surface. For each particle, a fixed, accumulated total nano-tube diameter of 2.5 x 10^{-7} m was used in this work. If it is assumed that an average nano-tube has a diameter of 20 nm, then 2.5 x 10^{-7} m would correspond to about 156 nano-tubes per particle or 70 nano-tubes/mm^2. All values listed here are arbitrary; they were selected based on the fact that these values could reproduce the limited available data reasonably well in a first evaluation. It was also assumed that released activities reported in German irradiation test reports were actual measured activities on collection cups used in the experiments at the end of the irradiation period. This would overestimate release fractions since ^{109}Ag activation to ^{110m}Ag on plated-out surfaces would be far more than neutronic removal of ^{110m}Ag from these surfaces. These effects were included in the calculation model.

Test results and corresponding NTF are listed in Table 2. In total 12 irradiation tests have been analysed. From this an average NTF value and a 95% confidence interval have been determined to be used as input into ^{110m}Ag release calculations for a PBMR core. Experiment R2-K12/1 had an exceptional high silver release and could be considered an outlier. Considering all test results, an average NTF value of 7.51% was derived. By excluding the possible outlier R2-K12/1, the NTF value decreases to 4.71% [8].

The NTF value of 7.51% was used in an MVR calculation model to compare with a simplified diffusion model (recoil and sorption ignored) and experimental measured data. The diffusion model used currently accepted diffusion constant and activation energies described in the literature [2]. Fractional releases for both MVR and diffusion calculations are listed in Table 2 and presented in Figure 9.

It can be seen that at temperatures below 1 050 °C, MVR calculates slightly higher releases than diffusion, but for temperatures above 1 150 °C, both models over-predict silver release, with diffusion predicting the highest releases. This is because of the possible outlier R2-K12 being included in the NTF value and the strong temperature-dependence of the silver diffusion coefficient in SiC. Even though diffusion generally predicts higher releases, in the critical region 970 °C to 1 120 °C MVR predicts slightly higher releases. The MVR and diffusion models used in this evaluation concentrated on SiC retention and ignored sorption effects. This causes a difference of up to one order of magnitude in the estimated source term by MVR and PBMR diffusion calculation models. This raised the concern that the ^{110m}Ag source term may be underestimated for PBMR safety analyses which in turn led to the revaluation of the diffusion model described in the next paragraph.

Table 2: MVR (NTF) and Diffusion Evaluation

Experiment	Irradiation Time (EFPD)	Maximum Fuel Temperature	FIMA (%)	NTF (%)	Fractional Silver Release	MVR Fractional Release	Diffusion Fractional Release
R2-K12/1	308	1 100	11.1	38.26	3.30E-02	6.42E-03	7.48E-03
R2-K12/2	308	1 280	12.4	1.37	1.40E-02	8.19E-02	1.77E-01
R2-K13/1	517	1 170	10.2	3.74	3.90E-02	8.17E-02	1.22E-01
R2-K13/4	517	980	9.8	2.46	2.70E-03	8.29E-03	7.08E-03
HFR K3/1	359	1 200	7.5	0.37	2.20E-03	4.61E-02	5.18E-02
HFR K3/4	359	1 220	9	3.52	1.80E-02	3.94E-02	7.32E-02
FRJ2 K13/1	396	1 125	7.5	5.75	1.90E-02	2.49E-02	1.64E-02
FRJ2 K13/2	396	1 150	8	5.47	2.00E-02	2.76E-02	2.83E-02
FRJ2 K13/3	396	1 150	7.9	4.237	1.70E-02	3.04E-02	3.05E-02
FRJ2 K13/4	396	1 120	7.6	13.25	3.90E-02	2.17E-02	1.46E-02
FRJ2 K15/1	533	970	14.1	10.54	7.50E-04	5.34E-04	3.99E-04
FRJ2 K15/2	533	1 150	15.3	1.12	3.20E-03	2.18E-02	1.00E-01

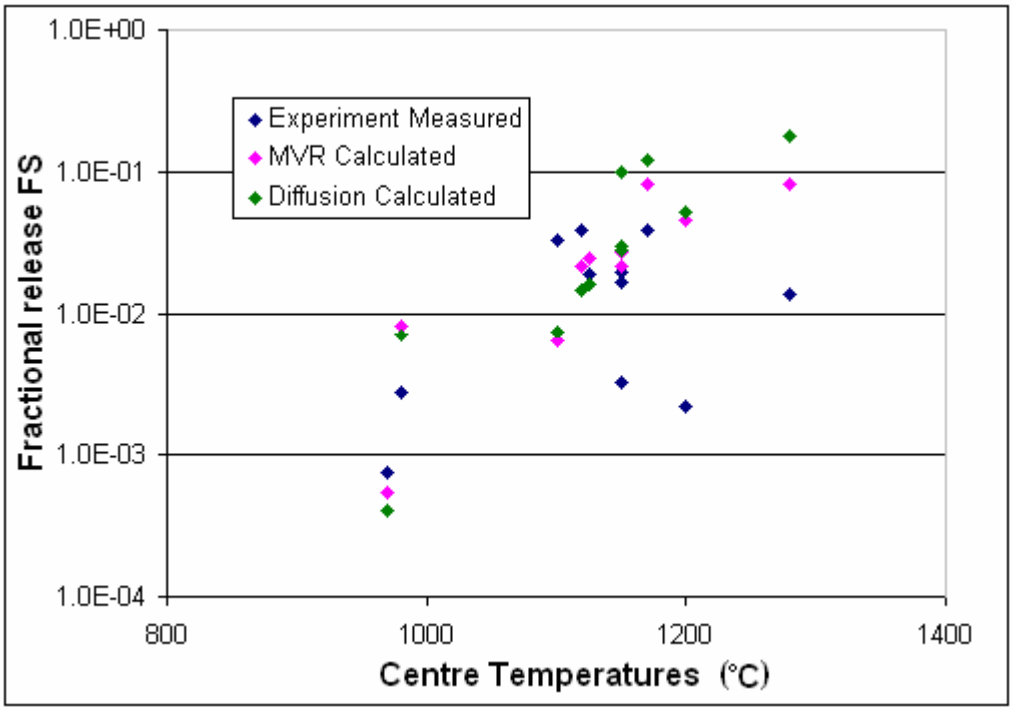

Figure 9: Fractional ^{110m}Ag Release: Experiment vs. MVR vs. Diffusion

4.3 Diffusion Model

After the interesting results of the MVR evaluation, it became clear that the diffusion model used at PBMR must be re-evaluated and proven not to underestimate the ^{110m}Ag source term under all operating conditions or be replaced by a MVR-type calculation model. However, no verification and validation (V&V) had been performed on the MVR calculation model, which would include a proper in-depth evaluation of all applicable German irradiation tests. It was decided to evaluate applicable German irradiation tests first with an updated diffusion calculation model based on a first estimate evaluation of all data. This is to be followed by an in-depth evaluation of all the German irradiation results by either a diffusion model (if the first estimate evaluation showed diffusion to be acceptable) or a MVR calculation model (should diffusion be found unacceptable). The first estimate evaluation is described in the following paragraph.

4.3.1 First estimate evaluation

A first evaluation of all data was performed to get a first estimate of all transport parameters to be used during detailed evaluations of each selected irradiation test [24]. In Figure 10 fractional releases for 31 selected irradiation tests (from Table 1) are plotted against maximum centre temperatures achieved during irradiation.

All data points below 1 100 °C were fitted by one line and all data points 1 100 °C and higher by a second fitting line. These fitting lines represent the average of the data for the two temperature regimes and provide guidelines as to where a diffusion curve should go through the plotted experimental data. All data points are plotted and are considered equally important for this first estimate.

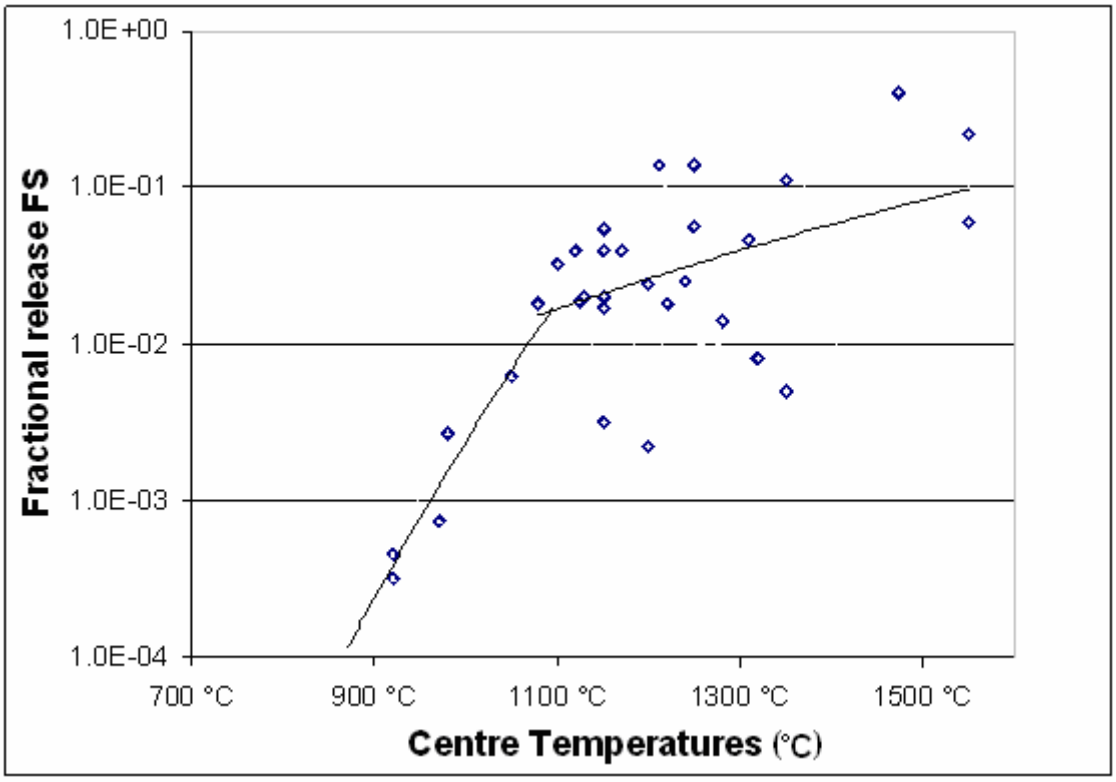

Figure 10: Fractional ^{110m}Ag Release after Irradiation

Based on analyses of natural silver contamination in sphere cups and capsules [25] and the expected natural silver contamination in matrix material, a natural silver contamination of 0.8 ng/g Ag/C was suggested [26]. Approximately 48.7% of natural silver is ^{109}Ag and the graphite cups housing each test sphere are assumed to be of equal volume. It was also decided to use the standard verified GETTER routines and to include all contaminations in the matrix material contamination of the fuel. Considering the above, a slightly conservative 8 x 10^{12} atoms/cm^3 ^{109}Ag/C was used as GETTER input.

The majority of released silver is released as fission product ^{109}Ag before being activated to ^{110m}Ag. Released ^{109}Ag is deposited on cups and capsules that house the test spheres. Contrary to what happens in a reactor, released ^{109}Ag is not removed from the neutron flux field and deposited in the cooler areas of the main power system, but remain in the neutron flux field. ^{109}Ag continues to be activated in the cups and capsules at a similar rate to what ^{109}Ag is activated in the fuel elements.

Fractional release is experimentally determined by comparing the ^{110m}Ag activity on the cups and capsules that house the test spheres and the total ^{110m}Ag produced during irradiation. The ratios of ^{109}Ag released to ^{109}Ag produced (the ^{109}Ag fractional release) and ^{110m}Ag released to ^{110m}Ag produced (the ^{110m}Ag fractional release) is therefore the same as long as the released silver nuclides remain in the same irradiation field as the fuel. The differences between ^{109}Ag and ^{110m}Ag absorption cross sections and neutron flux spectra in the fuel and cups cause differences between production of ^{110m}Ag from ^{109}Ag of less than 10% [27]. This is less than the expected measurement uncertainty of ^{110m}Ag on cups and capsules or the calculated ^{110m}Ag inventory in the test spheres (~10%), cross section uncertainties (~20%) and flux uncertainties (10%) [27]. Therefore this assumption is adequate as a first estimate. It was conservatively assumed that fuel spheres were irradiated at a constant centre temperature and fission power and coolant temperatures were adjusted accordingly.

A diffusion curve is drawn by using the existing accepted diffusion coefficient of Ag in SiC (IAEA data [2]) and the current diffusion calculation model used at PBMR. A new calculation model using parameters and models used to describe fission product recoil from fission sites, diffusion through UO_2, PyC and matrix materials and desorption from the fuel surface as was suggested in Chapter 3, was developed.

The SiC diffusion coefficient was adjusted so that a diffusion curve based on the new diffusion calculation model would follow the two fitted lines in Figure 10 as closely as possible. The two diffusion lines are shown in Figure 11. The new diffusion curve that matches the fitted lines as closely as possible should be considered a best estimate curve as it fits the average of the available data. Similarly, a new design limit diffusion curve was drawn by setting the SiC diffusion coefficient so that 95% of the experimental data lies below the diffusion curve. The design limit also includes the upper limit uranium and thorium fuel contamination, and design diffusion coefficients for PyC and matrix material transport. Both the best estimate and design limit curve show an inflection at approximately 900 °C. This the point where the contribution of the natural silver contamination to the silver source term becomes significant.

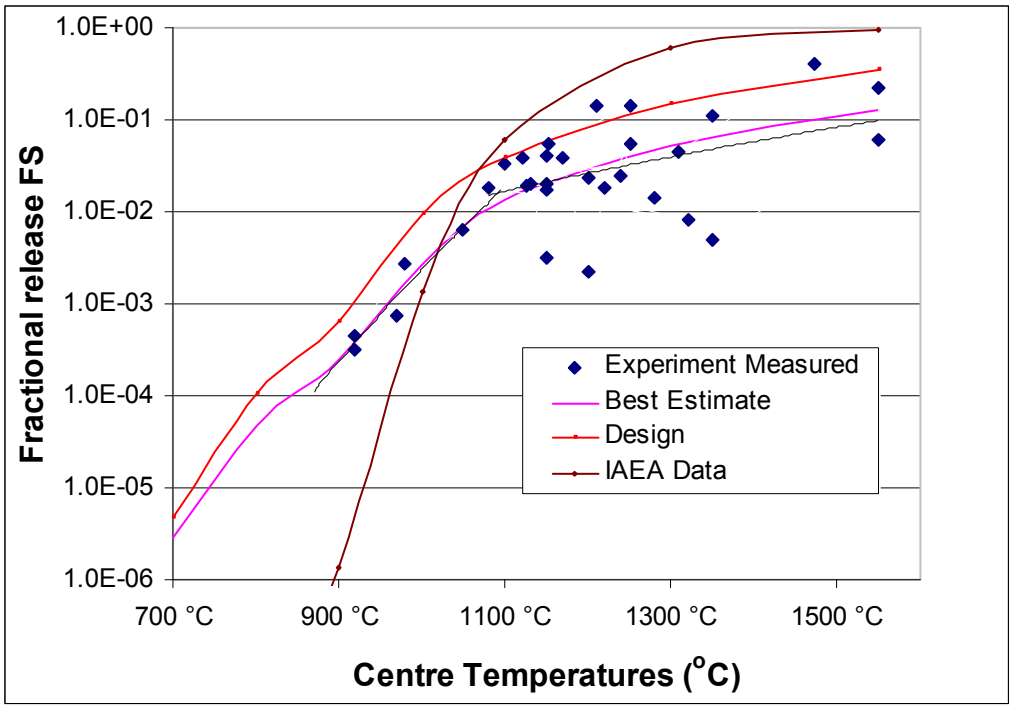

Figure 11: Fitted IAEA, and First Estimate Best Estimate and Design Limit Curves

The biggest difference between the old diffusion curve and the two new curves are the SiC diffusion constant and activation energy and are as follows:

IAEA best estimate [2]: $D = 3.60 \times 10^{-9} e^{-215/RT}$ m^2s^{-1}

First estimate best estimate: $D = 1.70 \times 10^{-15} e^{-63/RT}$ m^2s^{-1}

First estimate design limit: $D = 1.30 \times 10^{-14} e^{-75/RT}$ m^2s^{-1}

The very small activation energy for silver diffusion appears very radical and seems to contradict the findings of previous work [3], but it is much less drastic than the suggested molecular vapour transport release model. The new suggested SiC diffusion coefficient from this first estimate analyses is plotted with the current IAEA best estimate diffusion coefficient as a function of temperature in Figure 12. Figure 11 shows that a carefully selected set of diffusion constants can in principle simulate the irradiation tests results. This analysis showed that diffusion theory remains a viable option to model transport of silver and that further detailed analyses of all applicable irradiation tests are required.

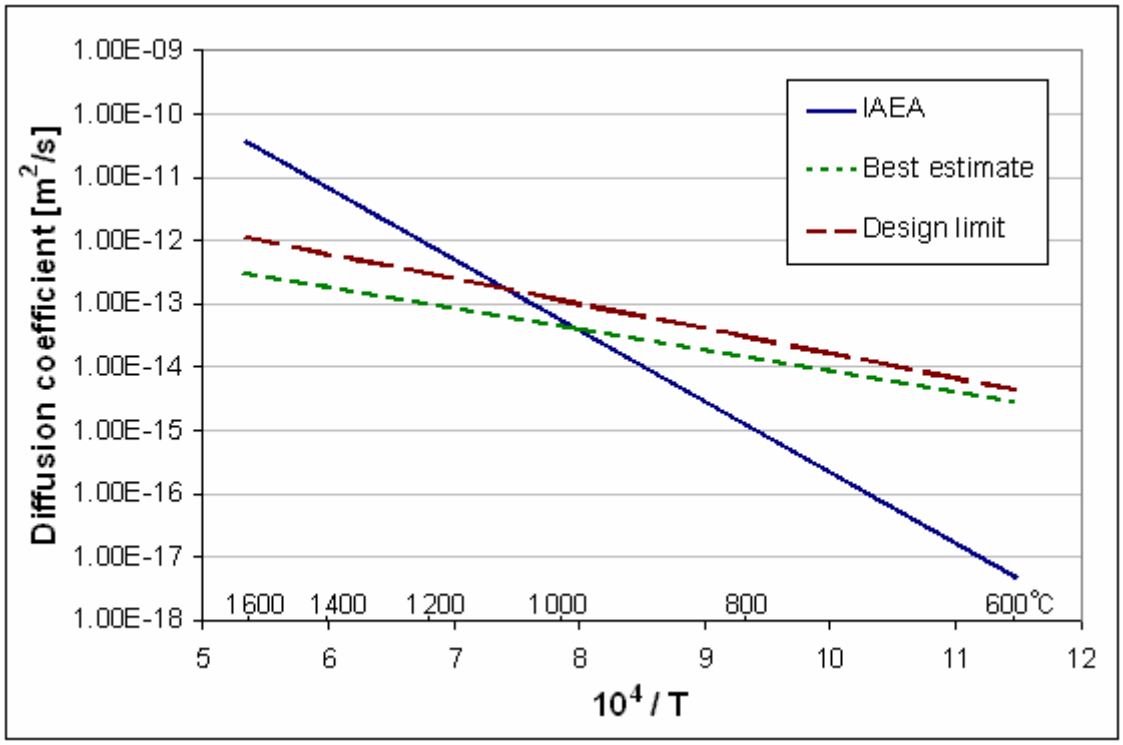

Figure 12: IAEA and First Estimate Best and Design SiC Diffusion Coefficients